

Hierarchical Reinforcement Learning for Sensor-Based Navigation

Christopher Gebauer

Maren Bennewitz

Abstract—Robotic systems are nowadays capable of solving complex navigation tasks under real-world conditions. However, their capabilities are intrinsically limited to the imagination of the designer and consequently lack generalizability to initially unconsidered situations. This makes deep reinforcement learning especially interesting, as these algorithms promise a self-learning system only relying on feedback from the environment. Having the system itself search for an optimal solution brings the benefit of great generalization or even constant improvement when life-long learning is addressed. In this paper, we address robot navigation in continuous action space using deep hierarchical reinforcement learning without including the target location in the state representation. Our agent self-assigns internal goals and learns to extract reasonable waypoints to reach the desired target position only based on local sensor data. In our experiments we demonstrate that our hierarchical structure improves the performance of the navigation agent in terms of collected reward and success rate in comparison to a flat structure, while not requiring any global or target information.

I. INTRODUCTION

In the last decade the consumer market reveals an increasing demand for mobile robots to assist a human user in a divers set of housekeeping tasks. While the general benefit for the consumer is out of question, most systems have a major limitation: They do not improve their behavior over time and are poor at generalization, in particular when facing situations that were not considered beforehand. The idea of machine learning is very inspiring in that case, because it allows to search for the optimal solution and improve it over time in case of unconsidered situations or changes in expectation. Especially, deep reinforcement learning (RL) is appealing as it does not require the optimal solution to learn from but only feedback that reflects its current behavior.

For robot navigation the current state of the art uses global information and is aware of the position of the target [1]. For reinforcement learning based approaches, this information is used during runtime to provide a detailed insight to the surrounding obstacles, such as a map and waypoints of the global path [2] or the heading direction of the surrounding humans [3]. However, inspired by Sutton [4] we are interested in the capabilities of a reinforcement learning agent that is not provided with any goal-oriented or global information to see how far the limits can be pushed, while still solving the navigation task. Recently, Mirowski *et al.* [5] trained a navigation agent without providing target information to the agent with very promising results. However, the authors

All authors are with the Humanoid Robots Lab, University of Bonn, Germany. This work has partly been supported by the German Research Foundation under Germany's Excellence Strategy, EXC-2070 - 390732324 (PhenoRob).

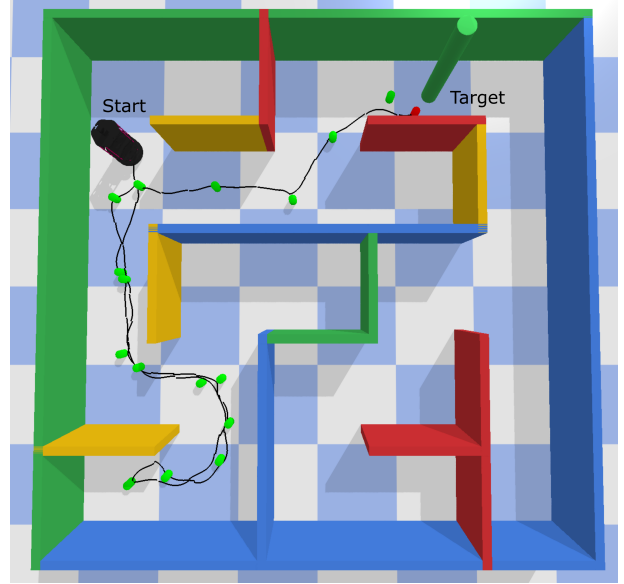


Fig. 1: We train a hierarchical reinforcement learning agent to identify and reach its target only based on local sensor information. At the beginning of the training the agent is not aware what the target is and where it is placed. The hidden target (green pole) is successfully identified in a randomly generated maze by our agent, as indicated by the black trajectory. The green markers represent the internal goals generated by the agent.

select the control signals from a discrete action space. This simplifies the task, as the required exploration in the action space is reduced, but also limits the fineness of the robot's motion capabilities due to discretization.

Therefore, in this paper we present an approach to the sensor-based navigation problem in continuous action space. To address the complexity of the continuous action space we deploy a hierarchical agent structure [6], which distributes the exploration across multiple layers. We consider the task, where the target is hidden in an unknown environment. The target is uniquely identifiable, but unknown at the beginning of the training. This motivates the idea of an agent that is capable of assigning its own waypoints based on intrinsic motivation. Even though our formulation is not limited to a specific sensor, we only use a 2D lidar scanner as it is a reasonable choice for indoor navigation. To efficiently incorporate the high-dimensional information from the 2D lidar sensor we pretrain an autoencoder [7], which provides a dense state representation to the hierarchical agent.

Our main contribution is a generic agent structure that is capable of solving a navigation task in continuous action space without relying on any information provided by a human expert. We achieve this by applying a hierarchical

structure and distribute the required exploration across the layers. Our agent learns to reach an arbitrary target in an unknown environment only based on local sensor data. We train the entire agent at once and demonstrate its performance in two different environments, see Fig. 1 and Fig. 3. The experiments show the seriously increased performance of our hierarchical structure in comparison to a flat agent regarding the collected reward and success rate. Furthermore, we transfer the trained agent into a real-world scenario to prove the concept under realistic conditions.

II. RELATED WORK

While classical approaches for robot navigation, e.g., the dynamic window approach [8], work very well in many situations [1], it is much more desirable to have the algorithm search for the optimal solution by itself [4]. To address this idea Pfeiffer *et al.* [9] used a target-driven approach that learns to steer a mobile robot collision-free to reach a relative goal pose. Furthermore, Tai *et al.* [10] combined reinforcement learning with a classical global path planning algorithm to reach a target position. Stein *et al.* [11] on the other side, improved the global path planning by incorporating machine learning in the process of evaluating possible future subgoals. The authors proposed to predict the expected cost for each of the possible subgoals and decrease the overall path length by choosing the most promising ones.

In contrast to the approaches above, Jaderberg *et al.* [12] introduced an agent that solves a robot navigation task end-to-end by only providing sensor information. The agent has to explore an unknown maze to find hidden targets. Mirowski *et al.* [5] extended this approach by improving the structure of the agent. Even though learning on raw sensor data works, Sax *et al.* [13] showed that a well-defined state space is crucial when addressing complex navigation tasks and uses the latent space of different pre-trained autoencoders. Chaplot *et al.* [14] proposed an object-oriented navigation agent based on semantic exploration. This helps to understand where certain objects are more likely to be found and therefore improves the navigation capabilities. While all these approaches seem promising in general, they are limited to a discrete action space and Dhiman *et al.* [15] questioned if such agents are capable of solving the navigation problem with comparable performance to classical hand-crafted approaches. Whaid *et al.* [16] trained in continuous action space and compare different observations for a flat agent structure. The authors showed that lidar information have significant impact on the performance in learning-based navigation tasks.

To increase the capabilities of an agent in complex tasks Vezhnevets *et al.* [17] introduced a hierarchical agent based on deep reinforcement learning, where a high-level manager sets subgoals on low frequency and a worker executes low-level actions at each time step following these subgoals. Levy *et al.* [6] introduced off-policy corrections based on hindsight experience replay [18] and reformulated the hierarchical approach to an arbitrary number of hierarchical layers. The authors demonstrated the effectiveness in the context of

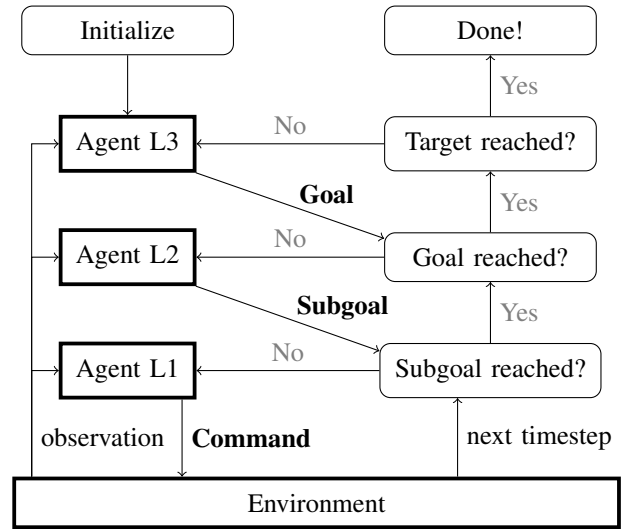


Fig. 2: The information flow of our hierarchical reinforcement learning structure for one mid-level agent, i.e., $I = 3$. The algorithm is initialized on the top left. The top-level agent (L3) provides a relative goal position based on the provided observation by the environment, with the purpose to reach the hidden target. Based on the provided goal and a current observation the mid-level agent (L2) provides a subgoal. The low-level agent (L1) sends commands, i.e., translational and rotational velocities, to the environment, based on the provided subgoal and a current observation.

robot navigation for up to three hierarchical layers. However, the agent receives the position of the goal as part of the state representation. Li *et al.* [19] introduced a hierarchical approach to simultaneously control a robot arm and the base it is attached to. While this again demonstrates the incredible capabilities of hierarchical structures, the state contains the location of the goal. Wang *et al.* [20] went a step further and demonstrated that a hierarchical agent is capable of solving a navigation task only relying on local sensor information. The authors used a model-based reinforcement learning approach to find an optimal meeting point for two mobile robots without centralized communication.

In this paper, we introduce a hierarchical reinforcement learning approach to solve the problem of robot navigation in unknown environments. As Whaid *et al.* [16] showed that lidar is crucial for navigation we use this type of sensor data, even though our formulation is not bounded to this sensor. In contrast to the related work, in particular Levy *et al.* [6], we do not provide any target information within the state space. This motivates the idea of having the agent identify its own internal goals based on observations and experience from the past training.

III. OUR APPROACH

In this section we discuss our approach in detail. At first we give the preliminaries regarding reinforcement learning and the general extension to the hierarchical structure. Next, we describe our agent and its structure in the context of a generic navigation task, as well as the reward function. Finally, we discuss the countermeasures for the instabilities due to concurrent training of all layers.

A. Preliminaries

We define our reinforcement learning setup as a partially observable Markov Decision Process (POMDP) [21] in a hierarchical structure of I layers. The hierarchical POMDP is a tuple of $(\mathcal{S}, \mathcal{O}, \mathcal{A}, \mathcal{R}, \mathcal{T}, \gamma, I)$ components described below. The state $s_t \in \mathcal{S}$ describes the distinct and explicit configuration of the environment in timestep t and is not directly accessible for the agent. Before proceeding, we simplify the full hierarchical POMDP into a layer-wise representation $(\mathcal{S}, \mathcal{O}_i, \mathcal{A}_i, \mathcal{R}_i, \mathcal{T}_i, \gamma, \Delta t_i)$, where i represents the current layer and denotes from now on layer-dependent quantities. With this step we assume that the structure of the underlying process in each layer is identical. Furthermore, it outlines that each layer operates on a different time scale Δt_i , i.e., a complete episode for layer i equals one time step for layer $i + 1 \leq I$.

Proceeding with layer i , the agent receives in timestep t_i an observation $o_{t,i} \in \mathcal{O}_i$ and selects an action $a_{t,i} \in \mathcal{A}_i$ according to its policy $\pi(\theta_i) : \hat{\mathcal{O}}_i \rightarrow \mathcal{A}_i$, where θ_i parametrizes the policy. The extended observation space $\hat{\mathcal{O}}_i$ for $i < I$ is computed by combining the observation space with the current action from the layer above $f_i : \mathcal{O}_i \times \mathcal{A}_{i+1} \rightarrow \hat{\mathcal{O}}_i$. For $i = I$ it is equal to the observation space itself, i.e., $\hat{\mathcal{O}}_I = \mathcal{O}_I$. After action $a_{t,i}$ has been executed, the agent receives a reward $r_{t,i} \in \mathcal{R}_i$ and the next observation $o_{t+1,i}$. The transition is selected according to the state-transition function $\mathcal{T}_i : \mathcal{S} \times \mathcal{A}_i \times \mathcal{S}$. The optimal policy $\pi(\theta_i)$ maximizes the discounted reward $R_{t_i} = \sum_{j=0}^{T_i} \gamma^j r_{t_i+j\Delta t_i}$, where T_i are the number of steps to reach the final timestep of the current episode in layer i and $\gamma \in [0, 1]$ is the discount factor.

B. Background

Before explaining the hierarchical structure in detail, we will shortly define the capabilities of the considered mobile base. As we explicitly avoid any global information, the agent is designed to solve general navigation problems with an observable target. The target can be an arbitrary object, e.g., a lost key ring or even a hiding human, and does not need to be known for the agent at the beginning of the training. This information is obtained during the training using the provided reward. Therefore, it needs to be uniquely recognizable by the agent using its sensor.

The mobile robot observes the external environment using a local sensor, e.g., lidar sensors or RGBD-cameras, and measures its internal state based on odometry. We refer to these observations as o_{ext} and o_{int} , respectively. The internal measurement includes a pose measurement in Cartesian space without localization. That means we only consider the relative offset to a recent, nearby measurement and assume a neglectable error, because no accumulation can take place.

C. Agent Structure

In this section we will introduce our hierarchical agent by dividing it into three different layer classes. The overall structure of the hierarchical agent is visualized in Fig. 2 for $I = 3$. The highest layer has the purpose to address the navigation task with high-level abstraction, i.e., finding the

hidden target within the unknown environment by proposing reasonable, internal goals. All other layers have the purpose to reach this goal. We define the action for this layer to be a relative position in Cartesian space, which we refer to as *goal*. To be able to avoid any global information, only the external observation is used as input:

$$a_{t,I} = \pi(o_{ext,t,I}, \theta_I) \quad \text{and} \quad d_I = p_I(o_{ext,t,I}, \theta'_I)$$

The quantity d_I signalizes if the target has been reached. This either has to be provided externally, e.g., when running under supervision, or a predictor p_I with its parameters θ'_I is trained on past experience using the external observation.

The next class of layers represents the entire middle of the hierarchical structure and therefore, is present $(I - 2)$ -times. It breaks down the distant goal into smaller subgoals to reach. In addition to the relative position in Cartesian space this layer can contain preferred velocities, i.e., to represent slowing down in narrow areas. In the following we will refer to the combination of both as *subgoal* of layer i . As input we use the external observation, which is layer-dependent to allow any data-augmentation if desired, e.g., reducing the line of sight to increase the attention for nearby obstacles:

$$a_{t,i} = \pi(o_{ext,t,i}, prog_i, \theta_i) \quad \text{and} \quad d_i = p_i(prog_i) \\ \text{with} \quad prog_i = f_i(o_{int,t}, a_{t,i+1}) \quad \text{for} \quad i \in [2, \dots, I-1]$$

Additionally, based on the internal state and the action from the layer above a progress is computed, which is used as input for the policy. In our case we compute the progress by transforming the position of the (sub-)goal into the current base-frame of the mobile robot, i.e., providing its current relative position. The quantity d_i signalizes if the relative position of the (sub-)goal from the layer above has been reached and is computed based on the progress.

The lowest layer is directly communicating with the mobile base by sending control signals in the form of translational and rotational velocities. It receives only the progress computed based on the subgoal from the layer above and the internal observation:

$$a_{t,1} = \pi(prog_1, \theta_1) \quad \text{and} \quad d_1 = p_1(prog_1) \\ \text{with} \quad prog_1 = f_1(o_{int,t}, a_{t,2})$$

We do not pass the external observation, because the subgoals are learned to be reachable collision-free, due to the received penalties when collisions occur. That means, the agent automatically learns to set subgoals such that the lowest layer is capable of reaching those collision-free. The quantity d_1 signalizes if the position of the subgoal $a_{t,2}$ has been reached and is computed based on the progress.

D. Reward Function

We divide the reward into two categories: An external reward provided from the environment r_{env} and an intrinsic reward with two different origins, based on which layer is receiving it. The external reward from the environment r_{env} is explicitly designed to be sparse. A greater positive reward is provided, when the final target is discovered and a smaller

penalty when a collision occurs. In all other timesteps this reward is zero. We only provide this reward to the layers that also use the external observations from the sensor. For the layers that receive a (sub-)goal, the intrinsic reward is based on the progress towards this (sub-)goal r_{prog} . It consists of a smaller dense reward, e.g., the distance change normalized by the initial distance to the (sub-)goal, and a greater reward when the internal (sub-)goal is reached. To have an intrinsic reward for the top layer that does not receive any (sub-)goal, we grant a small reward r_{act} correlating with the magnitude of the action to emphasize doing anything. In our experiments we always chose the environment reward r_{env} to be a magnitude above the intrinsic motivation, as it increases the convergence speed. The reward function is summarized as follows:

$$r_t = \begin{cases} r_{env} + r_{act} & , i = I \\ r_{env} + r_{prog} & , i \in [2, \dots, I - 1] \\ r_{prog} & , i = 1 \end{cases}$$

E. Training Stability

In this section we discuss the countermeasures for the instability when training the full hierarchical agent at once. The necessity becomes obvious, when focusing on the state-transition probability \mathcal{T}_i for $i > 1$. The quantity itself is defined stationary, but will change when the policy of the layer below is adopted. Nachum *et al.* [22] did an excessive search for off-policy corrections in hierarchical reinforcement learning and showed that simply relabeling the interactions from the environment works better than any analytical solution. Therefore, we use the hindsight actions introduced by Levy *et al.* [6]. The key idea is to assume, wherever the agent ended up was the intended, internal goal position. This correction can be done either for the layer receiving the goal, to experiencing the reward for reaching it, or for the layer providing the goal, to experience an optimal lower policy.

However, for the top layer the target cannot be changed, as it is part of the sensor data and not provided directly. To still have this layer experience its actions independent from the capabilities of the lower layers, we added an additional interaction, which we refer to as *imagined interaction*. We check what the reward would be if the desired, internal goal would have been reached. As we are in simulation and our reward function does not depend on the behavior of any hierarchical layer below, we can directly compute the next observation and the reward. We will demonstrate its effectiveness by training the top level agent only based on imagined interactions in the experimental evaluation.

IV. EXPERIMENTAL EVALUATION

In this section we evaluate our approach in the context of navigation capabilities within simulation and transfer it into a real-world scenario. At first, we specify our setup, including the agent and the environments. Next, we show the performance when only training the top agent using the imagined interactions, explained in Sec. III-E. Finally,

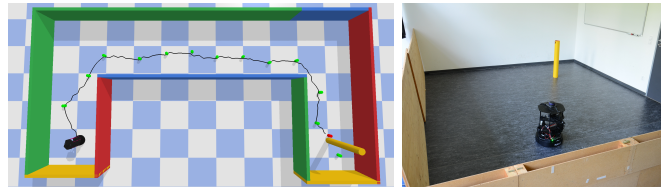


Fig. 3: Visualization of the *rooms* environment. **Left:** Trajectory in simulation, the green markers represent the internal goals from our agent. **Right:** Reproduction of an environment in our lab.

we demonstrate the performance when the entire agent is trained at once and transfer the trained agent into a real-world scenario.

A. Setup

In this section we introduce the environments we evaluate our hierarchical structure in. Furthermore, we specify all details of the agent, as well as the preprocessing we apply to the raw sensor data.

Environment. We test our agent in two environments with different degrees of complexity. As external sensor we use a 2D lidar scanner with a maximal range of 10 m. Both environments consist of interconnected corridors or rooms with one pole representing the hidden target. The position of the robot and of the target is drawn randomly at the beginning of each episode. Furthermore, we always ensure that the robot starts away from the target. The first environment is explicitly designed to be simple and consists of up to three interconnected rectangular rooms or corridors, see Fig. 3 (left). The width and length of the rooms as well as the composition are randomly drawn at the beginning of each episode. We will refer to this environment as *rooms*. The second environment consists of a random maze, which we refer to as *mazes*. The composition is drawn randomly, but the size is always fix. The environment is visualized in Fig. 1. For training we apply curriculum learning [23] in both environments and increase the difficulty step by step, i.e., the target is easier to discover in early stages of the training. An episode ends, when the target is discovered (signalized by the environment), a collision occurs, or the maximal number of steps for the top layer is reached. If a different layer reaches its maximal number of steps, a new goal is provided to that layer. We apply the reward as described in Sec. III-D. For the simulation we used pybullet [24] and wrapped it with Gym [25].

Preprocessing. As mentioned before, we use a 2D-lidar sensor as external sensor and build our preprocessing pipeline upon our previous work [7], i.e., we convert raw lidar data into a local occupancy grid, which is encoded using a variational autoencoder (VAE) [26]. This has two benefits in contrast to autoencoding raw lidar scans. First, the reconstruction capabilities are significantly increased, which allows to reconstruct more accurately complex geometric shapes. Furthermore, the grid map can be cropped without any need of replacing the new out-of-range measurements. This reduces the information content provided to the agent,

when only information of nearby obstacles is required, and helps decreasing the size of the latent space.

Agent. In our experiments the goal is represented by the relative offset in x- and y-coordinates. For the highest level we use a maximal range of 1 m and 0.3 m for the middle layer. We use one mid-level layer, which leads us to a total number of three layers that will be trained in parallel. We decided to have at least one middle layer, because Levy *et al.* [6] showed an improved performance with an increasing number of layers. However, having too many layers makes the training unstable, therefore we did not increase the number of the middle layers further. The middle layer provides a target velocity in translational direction in addition to the relative waypoint to reach. For this layer we reduce the line of sight of the lidar sensor to 2 m, which still includes the position of the goal but already reduces the dimension of the latent space by a factor of 4. The lowest layer sends velocity commands in translational and rotational direction to the mobile base. All three agents are optimized with the twin delayed deep deterministic policy gradient (TD3) algorithm [27]. We parametrize all policies with small dense neural networks, consisting of two layers.

B. Top Layer Training

In this section we demonstrate the functionality of our imagined interaction from Sec. III-E by training the top-level agent. We do so by only updating the top-level agent based on these interactions, while the layer below are not present. That is possible, because the imagined interaction has the purpose to remove the dependency from the behavior of the layer below. Furthermore, we focus on testing different network configurations for the top-level agent. In particular, we compare the effect of concurrently continuing the training of the encoder weights with the agent and incorporating the reinforcement learning loss. Furthermore, we investigate the influence of adding recurrent layers to the structure or the agent, as suggested by Mirowski *et al.* [5].

As can be seen in Fig. 4, all of the configurations lead to similar results for the *rooms* environment. Only when training the encoder concurrently slight performance drops occur, which is originated in the fact that the agent constantly has to adapt to the changing state representation of the lidar scan. While it is neglectable in the case of the *rooms* environment, it is crucial for the *mazes* environment. Concurrently adopting to the changing state representation leads to a decreased overall performance in terms of collected reward. However, for lidar-based agents that is no problem, because data can easily be generated from any environment upfront, i.e., an encoder can usually be pretrained and kept fixed later on. In our previous work [7] we even noticed great generalization capabilities, which means that retraining is usually not required. Therefore, we will keep the encoder weights fixed when training the full agent in the next section. In contrast, the recurrent agent slightly improves the performance in the *mazes* environment, especially in the early stages of the training. However, the final performance is almost identical and has no effect in the *rooms* environment.

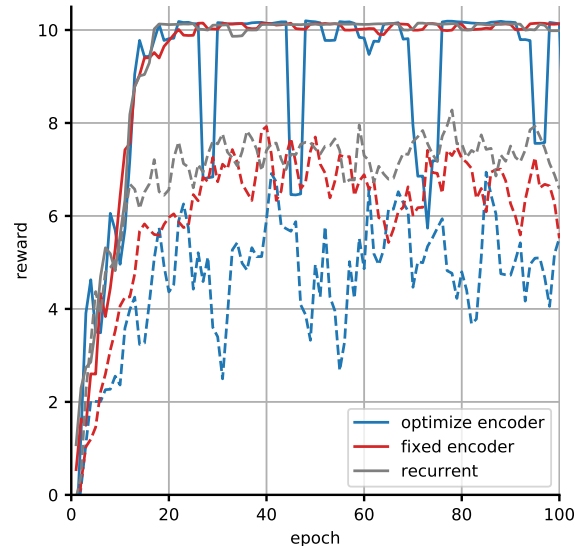


Fig. 4: Comparison of different setups of the network structure of the top-level agent in the *rooms* (solid) and *mazes* (dashed) environment: Collected reward over the number of epochs. Training the encoder concurrently (blue) leads to instabilities, while the recurrent layer (gray) has minimal effect. All curves are averaged over three runs and smoothed with a savgol filter [28].

Therefore, we choose for the sake of simplicity to use the dense network structure for the agent from now on.

C. Full Agent Training

In this section we evaluate the performance of our full hierarchical structure in two different environments, described in Sec. IV-A. For comparison we train an agent similar to Mirowski *et al.* [5] but in continuous action space, which we will refer to as *flat agent*. As we use the same pretrained encoder for the flat agent, we do not apply the auxiliary losses and, as described in the previous section, only rely on a dense network for the agent. As input we pass the encoded lidar scan, the current velocity, and the last action. The reward is chosen to be identical to the top layer as described in Sec. III-D.

As can be seen in Fig. 5, our agent outperforms the flat structure in both environments. In particular, the difference of the red line (our agent) and the gray line (flat agent) is of interest. While in the *rooms* environment (left) we achieve an increased reward in contrast to the flat agent, we more than doubled the reward in the *mazes* environment (right). However, we noticed instabilities in our agents performance, as soon as it starts to converge, i.e., random reward drops which do not disappear over the course of the training. We found the origin in the stabilizing countermeasures for the concurrent training, introduced in Sec. III-E. While these additional interactions are essential in the early stage of the training, they are not anymore as soon as the layer starts to converge. Therefore, we stop collecting these interactions when a certain reward is reached during evaluation. It is clearly visible that shutting off these interactions (red line) in the left plot lets the agent fully converge, while when

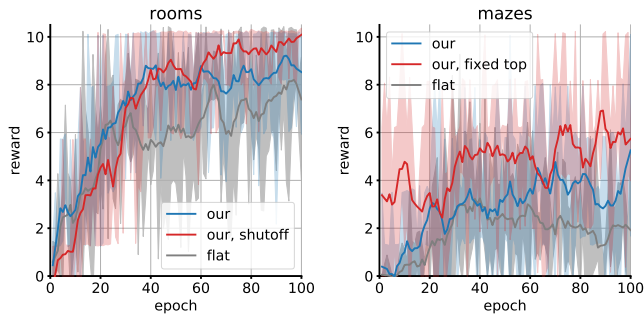


Fig. 5: Comparing our hierarchical agent in the *rooms* environment (left) and *mazes* environment (right) to the current state-of-the-art agent for local, sensor-based navigation [5]. The flat agent has only one hierarchical layer receiving the same input as our top layer. It is represented by the gray line. For our agent we plotted the reward of the highest layer (blue line), as it represents the overall performance and is directly comparable to the flat agent, due to the identical design of the reward. To reduce the instabilities for the *rooms* environment we shut off the hindsight/imagined interactions after a certain reward level is reached (red line, left). For the *mazes* environment we did the same, but also took a pretrained top-level agent and kept its weights fixed (red line, right). As can be seen, our hierarchical structure (blue and red) collects a higher reward than the flat agent. All curves are averaged over three runs and smoothed with a savgol filter [28].

keep collecting these interactions (blue line) the improvement stagnates. For the *mazes* environment we noticed even worse instabilities. While the performance is still above the flat agent, it is not comparable to the last section, when the top layer is trained independently of the layer below in Sec. IV-B. To overcome this we used the trained agent from the previous section and kept its weights fixed during training. Therefore, only the lower agents are trained. It can be seen that this increases the collected reward, especially in the early stages of the training.

As additional comparison we use the success rate of the agents. An episode counts as success if the hidden pole is reached without collisions and before the maximal number of timesteps is reached. In Tab. I it is clearly visible that our agent structure increases the success rate in all environments compared to the flat structure. However, when looking at the success weighted by the normalized inverse path length (SPL) [29] it becomes visible that the increased success rate comes with the price of less smooth trajectories, see also the resulting trajectories in Fig. 1 or our accompanying video. That is, because our SPL drops in comparison to the success rate relatively more than for the flat agent. Therefore, our trajectories are slightly longer, which is originated in the non-smoothness.

As we demonstrate with these experiments providing any global or target information can be avoided, using our hierarchical agent for navigation. Furthermore, in terms of collected reward and success rate we achieve an improved performance in comparison to the flat agent. However, looking at the success rates in Tab. I shows that navigation in complex environments such as *mazes* is still a challenging task.

Environment	Metric	Flat	Our	Random Walker
Rooms	Success	0.664	0.969	0.016
	SPL [29]	0.573	0.782	0.015
Mazes	Success	0.342	0.581	0.003
	SPL [29]	0.306	0.452	0.003

TABLE I: Success rate and SPL [29] for the *rooms* and *mazes* environment. Our agent seriously increases the success rate in comparison to the flat agent. The random walker, executing randomly drawn actions, is more than one magnitude below the flat and our agent. The reduced smoothness of our generated trajectory becomes noticeable, when looking at the SPL. Our SPL drops in comparison to the success rate relatively more than for the flat agent. Even though, SPL takes the success rate into account the non-smoothness leads to a longer trajectory and therefore alleviates the improved success rate. Furthermore, the lower success rates for *mazes* compared to *rooms* show that complex environments are still challenging when avoiding any global or target information. All values are obtained by averaging over 1000 trials.

D. Transfer to Real-World

In this section we demonstrate the transferability of our hierarchical agent when trained in simulation. Neither the encoder nor the agent itself have been trained on real-world data. As we only rely on a local sensor, in particular a 2D lidar scanner, and odometry, we do not have to apply any further supplementary algorithms for, e.g., localization. For evaluation we used the *rooms* environment and rebuilt a similar setup in our lab, see Fig. 3 (right). As mobile base we used a TurtleBot2i, as we have done in simulation. We placed the target and the robot on 15 different positions and started our hierarchical algorithm. To unambiguously determine the end of an episode, we let the algorithm run until the robot touched the target. In each episode our agent successfully reached the target, i.e., we achieved an success rate of 1.0. To further evaluate the performance in contrast to the simulation we evaluated the SPL [29]. In simulation our agent reached, while limited to the shape of the room in Fig. 3 (right), also an success rate of 1.0 and an SPL of 0.738 averaged over 1000 trials. In real-world the agent reached an SPL of 0.742 for the 15 trials mentioned above.

V. CONCLUSION

In this paper, we presented a novel hierarchical structure for generic navigation tasks using deep reinforcement learning. Our major focus is to avoid any global or target information in the state space for the agent. This motivates the idea of a self-assigning agent that discovers its own targets based on current sensor measurements. To further exploit the full capabilities of the mobile robot we use a continuous action space. This additionally simplifies the transfer to a real-world scenario as common mobile robots apply target velocities. We have shown that our entire agent can be trained at once. Furthermore, we demonstrated that our hierarchical structure clearly outperforms the flat agent in terms of collected reward and success rate. Overall, we showed the effectiveness of our hierarchical structure for navigation tasks in two different environments and demonstrated that the trained agent can easily be transferred into a real-world scenario.

REFERENCES

- [1] S. Macenski, F. Martin, R. White, and J. Ginés Clavero, “The marathon 2: A navigation system,” in *Proc. of the IEEE/RSJ Intl. Conf. on Intelligent Robots and Systems (IROS)*, 2020.
- [2] P. Regier, L. Gesing, and M. Bennewitz, “Deep reinforcement learning for navigation in cluttered environments,” *Proc. of the Intl. Conf. on Machine Learning and Applications (CMLA)*, 2020.
- [3] L. Liu, D. Dugas, G. Cesari, R. Siegwart, and R. Dubé, “Robot navigation in crowded environments using deep reinforcement learning,” in *Proc. of the IEEE/RSJ Intl. Conf. on Intelligent Robots and Systems (IROS)*, 2020.
- [4] R. Sutton, “The bitter lesson,” <http://www.incompleteideas.net/IncIdeas/BitterLesson.html>, 2019.
- [5] P. Mirowski, R. Pascanu, F. Viola, H. Soyer, A. J. Ballard, A. Banino, M. Denil, R. Goroshin, L. Sifre, K. Kavukcuoglu, D. Kumaran, and R. Hadsell, “Learning to navigate in complex environments,” *Intl. Conf. on Learning Representations (ICLR)*, 2017.
- [6] A. Levy, G. Konidaris, R. Platt, and K. Saenko, “Learning multi-level hierarchies with hindsight,” *Intl. Conf. on Learning Representations (ICLR)*, 2019.
- [7] C. Gebauer and M. Bennewitz, “The pitfall of more powerful autoencoders in lidar-based navigation,” in *arXiv preprint*, 2021.
- [8] D. Fox, W. Burgard, and S. Thrun, “The dynamic window approach to collision avoidance,” *Robotics Automation Magazine, IEEE*, 1997.
- [9] M. Pfeiffer, M. Schaeuble, J. I. Nieto, R. Siegwart, and C. Cadena, “From Perception to Decision: A Data-driven Approach to End-to-end Motion Planning for Autonomous Ground Robots,” *CoRR*, 2016.
- [10] L. Tai, G. Paolo, and M. Liu, “Virtual-to-real deep reinforcement learning: Continuous control of mobile robots for mapless navigation,” in *2017 IEEE/RSJ International Conference on Intelligent Robots and Systems (IROS)*, 2017.
- [11] G. J. Stein, C. Bradley, and N. Roy, “Learning over subgoals for efficient navigation of structured, unknown environments,” in *Proc. of the Conf. on Robot Learning (CoRL)*, 2018.
- [12] M. Jaderberg, V. Mnih, W. M. Czarnecki, T. Schaul, J. Z. Leibo, D. Silver, and K. Kavukcuoglu, “Reinforcement Learning with Unsupervised Auxiliary Tasks,” *CoRR*, 2016.
- [13] A. Sax, J. O. Zhang, B. Emi, A. R. Zamir, L. J. Guibas, S. Savarese, and J. Malik, “Learning to navigate using mid-level visual priors,” in *Proc. of the Conf. on Robot Learning (CoRL)*, 2019.
- [14] D. S. Chaplot, D. Gandhi, A. Gupta, and R. Salakhutdinov, “Object goal navigation using goal-oriented semantic exploration,” *Proc. of the Conf. on Neural Information Processing Systems (NIPS)*, 2020.
- [15] V. Dhiman, S. Banerjee, B. Griffin, J. M. Siskind, and J. J. Corso, “A critical investigation of deep reinforcement learning for navigation,” *arXiv preprint*, 2018.
- [16] A. Wahid, A. Stone, K. Chen, B. Ichter, and A. Toshev, “Learning object-conditioned exploration using distributed soft actor critic,” *arXiv preprint*, 2020.
- [17] A. S. Vezhnevets, S. Osindero, T. Schaul, N. Heess, M. Jaderberg, D. Silver, and K. Kavukcuoglu, “FeUdal networks for hierarchical reinforcement learning,” in *Proc. of the Intl. Conf. on Machine Learning (ICML)*, 2017.
- [18] M. Andrychowicz, F. Wolski, A. Ray, J. Schneider, R. Fong, P. Welinder, B. McGrew, J. Tobin, O. Pieter Abbeel, and W. Zaremba, “Hindsight experience replay,” in *Advances in Neural Information Processing Systems*, 2017.
- [19] C. Li, F. Xia, R. Martín-Martín, and S. Savarese, “Hrl4in: Hierarchical reinforcement learning for interactive navigation with mobile manipulators,” in *Proc. of the Conf. on Robot Learning (CoRL)*, 2020.
- [20] R. E. Wang, C. Kew, D. Lee, E. Lee, B. A. Ichter, T. Zhang, J. Tan, and A. Faust, “Model-based reinforcement learning for decentralized multiagent rendezvous,” in *Proc. of the Conf. on Robot Learning (CoRL)*, 2020.
- [21] L. P. Kaelbling, M. L. Littman, and A. R. Cassandra, “Planning and acting in partially observable stochastic domains,” *Artificial Intelligence*, 1998.
- [22] O. Nachum, S. S. Gu, H. Lee, and S. Levine, “Data-efficient hierarchical reinforcement learning,” in *Advances in Neural Information Processing Systems*, 2018.
- [23] Y. Bengio, J. Louradour, R. Collobert, and J. Weston, “Curriculum Learning,” in *Proc. of the Intl. Conf. on Machine Learning (ICML)*, 2009.
- [24] E. Coumans and Y. Bai, “PyBullet, a Python module for physics simulation for games, robotics and machine learning,” <http://pybullet.org>, 2016–2019.
- [25] G. Brockman, V. Cheung, L. Pettersson, J. Schneider, J. Schulman, J. Tang, and W. Zaremba, “OpenAI Gym,” 2016.
- [26] D. P. Kingma and M. Welling, “Auto-encoding variational bayes,” *Intl. Conf. on Learning Representations (ICLR)*, 2013.
- [27] S. Fujimoto, H. van Hoof, and D. Meger, “Addressing Function Approximation Error in Actor-Critic Methods,” in *Proc. of the Intl. Conf. on Machine Learning (ICML)*, 2018.
- [28] A. Savitzky and M. J. E. Golay, “Smoothing and differentiation of data by simplified least squares procedures,” *Analytical Chemistry*, 1964.
- [29] P. Anderson, A. X. Chang, D. S. Chaplot, A. Dosovitskiy, S. Gupta, V. Koltun, J. Kosecka, J. Malik, R. Mottaghi, M. Savva, and A. R. Zamir, “On evaluation of embodied navigation agents,” *arXiv preprint*, 2018.